Vol. 24 • No. 1 • January 3 • 2012

D10488

www.advmat.de

ADVANCED MATERIALS

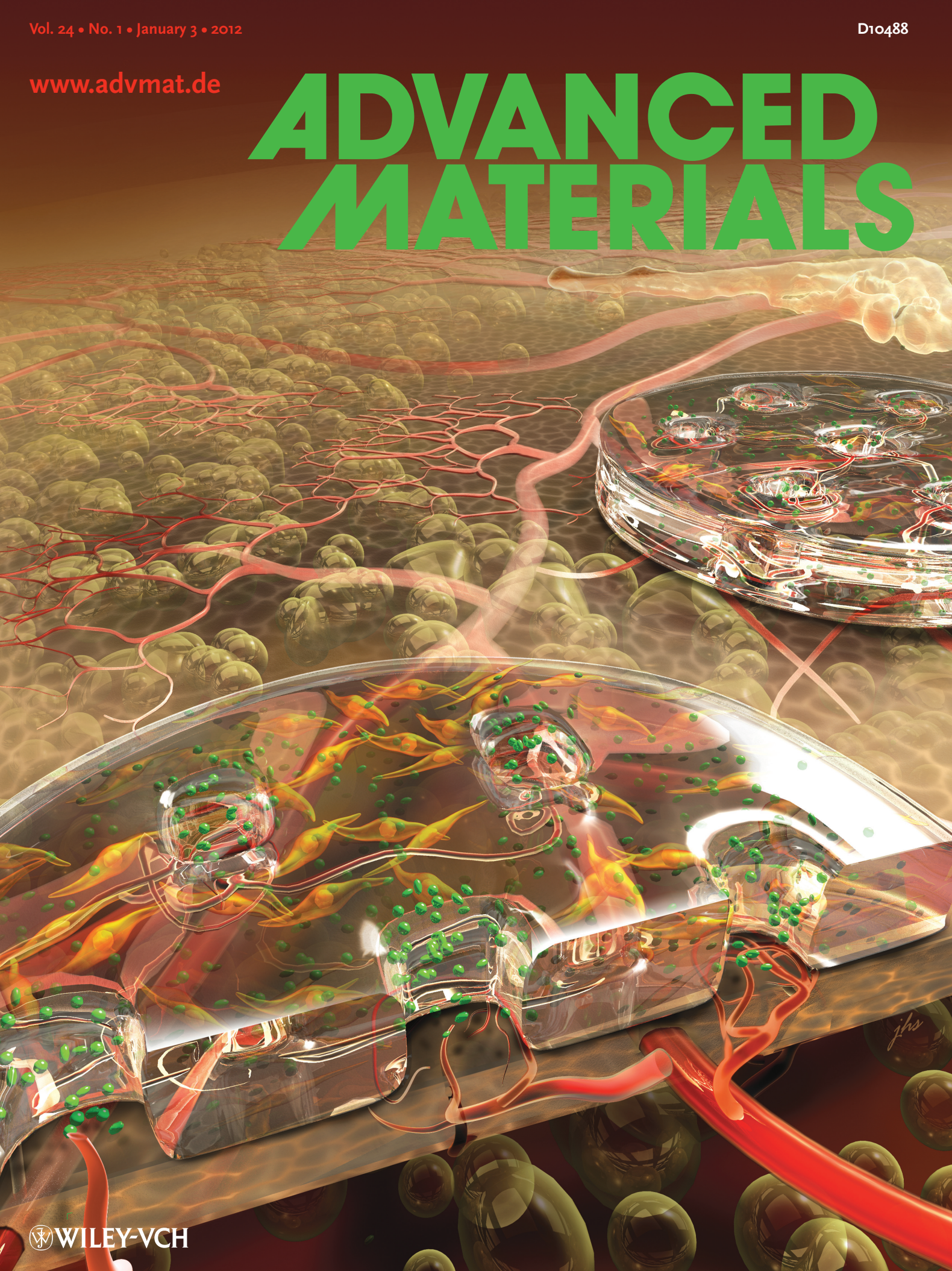

WILEY-VCH

"Living" Microvascular Stamp for Patterning of Functional Neovessels; Orchestrated Control of Matrix Property and Geometry

Jae Hyun Jeong, Vincent Chan, Chaenyung Cha, Pinar Zorlutuna, Casey Dyck, K. Jimmy Hsia, Rashid Bashir, and Hyunjoon Kong**

Neovessels play a critical role in homeostasis, regeneration, and pathogenesis of tissues and organs, and their spatial organization is a major factor in influencing vascular function.[1,2] Therefore, successful treatments of wounds, ischemic tissue, and tissue defects greatly rely on the ability to control the number, size, spacing, and maturity of blood vessels regenerated within a target tissue.[3,4] However, technologies to control the spatial organization of mature neovessels in vivo over physiologically relevant length scales are still lacking. Here, we present a study of a "living" microvascular stamp that releases multiple angiogenic factors and subsequently creates neovessels with the same pattern as that engraved in the stamp. The stamp consists of live cells that secrete angiogenic factors, an engineered hydrogel matrix that promotes cellular expression of angiogenic factors, and a three-dimensional (3D) geometry that localizes the angiogenic factors within the pattern. When the stamp was implanted on a target tissue, it created the desired pattern of neovessels based on 3D geometry of the stamp, allowing the control of the density and spacing of blood vessels. Analytical modeling and numerical simulations validated the experimental observations that the desired blood vessel patterns were formed under specific physical 3D designs of the stamp. The microvascular stamp developed in this study would serve to direct the emergent cellular behavior towards vascularization, improve the quality of revascularization therapies, and allow the vascularization of biological machines in vitro.

Prior studies have demonstrated that spatiotemporal distributions of multiple angiogenic growth factors can control growth direction and macro-scale spacing of neovessels. For example, polymeric scaffolds were developed by chemically attaching a growth factor-releasing layer with a growth factor-free layer, while varying layer thickness at millimeter scales.[4,5] In addition, certain membranes prepared with polytetrafluoroethylene have been clinically used to guide the growth of capillaries into tissue defects.[6] These results have advanced the state of the art, but many challenges remain unaddressed for precise patterning of functional blood vessels at the physiologically relevant sub-micrometer scale. Recently, various micropatterning, ink-jet printing, and microfluidic techniques have been reported to pattern molecules or cells on surfaces and in microfluidic environments.[7–9] These techniques have created patterned cell adhesion substrates, microfluidic devices or microfiber patches with chemotactic protein concentration gradients,[10] and cell-laden microporous tissue engineering scaffolds. However, these microfabricated devices still have to advance to regulate the desired spatial organization of mature and functional neovessels.

In response to the above challenges, we hypothesized that a construct assembled to sustainably release multiple angiogenic factors along a pre-defined micrometer-sized pattern would generate mature and functional neovessels with a desired pattern at an implant site. Therefore, the construct would allow us to control the area density and spacing of neovessels generated at the implant site. We examined this hypothesis by encapsulating cells that endogenously express multiple angiogenic growth factors into a rigid but permeable hydrogel of poly(ethylene glycol) (PEGDA) and methacrylic alginate (MA) (Figure S1a). Vertical microchannels with tuned diameter and spacing were incorporated into the cell-encapsulating hydrogel using a stereolithographic assembly (SLA) unit, in order to attain the local increase of angiogenic factors within the circularly patterned areas (Figure S1b and S1c). The resulting living microvascular

Prof. H. J. Kong
Department of Chemical and Biomolecular Engineering
University of Illinois at Urbana-Champaign
Urbana, Illinois 61801, USA
E-mail: hjkong06@illinois.edu
Prof. R. Bashir
Department of Electrical and Computer Engineering
University of Illinois at Urbana-Champaign
Urbana, Illinois 61801, USA
E-mail: rbashir@illinois.edu
Dr. J. H. Jeong, C. Cha, Prof. H. J. Kong
Department of Chemical and Biomolecular Engineering
University of Illinois at Urbana-Champaign
Urbana, Illinois 61801, USA
Prof. R. Bashir, V. Chan, Dr. P. Zorlutuna, Prof. K. J. Hsia
Department of Bioengineering
University of Illinois at Urbana-Champaign
Urbana, Illinois 61801, USA
C. Dyck, Prof. K. J. Hsia
Department of Mechanical Science and Engineering
University of Illinois at Urbana-Champaign
Urbana, Illinois 61801, USA
Prof. K. J. Hsia, Prof. R. Bashir, Prof. H. J. Kong
Micro and Nanotechnology Laboratory
University of Illinois at Urbana-Champaign
Urbana, Illinois 61801, USA
Prof. R. Bashir, Prof. H. J. Kong
Institute of Genomic Biology
University of Illinois at Urbana-Champaign
Urbana, Illinois 61801, USA

DOI: 10.1002/adma.201103207

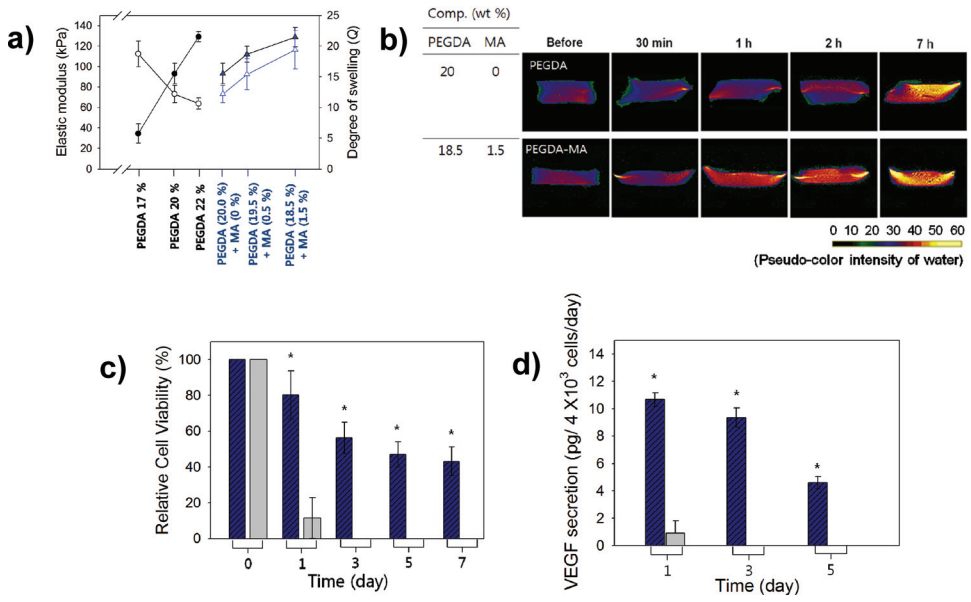

Figure 1. Characterization of stiffness and permeability of the PEGDA and PEGDA-MA hydrogels. a) The elastic modulus (▲) and decrease of the degree of swelling (△) of the pure PEGDA hydrogel were controlled with PEGDA concentrations. The elastic modulus (●) and degree of swelling (○) of the PEGDA-MA hydrogel were tuned with MA fraction at a given total polymer concentration of 20 %. b) Water protons diffused into the PEGDA hydrogel (upper row) and PEGDA-MA hydrogel (lower row) were visualized with MRI. Pseudo-color of MR images represents the relative peak intensity of water proton (see the scale bar under MR images). c) The viability of cells encapsulated in the PEGDA-MA hydrogel (■) and that encapsulated in the PEGDA hydrogel (■) (*p<0.05). The relative cell viability was quantified by normalizing the absorbance value of samples treated with MTT reagent to that measured at Day 0. d) The amounts of VEGF secreted by cells encapsulated within the PEGDA-MA hydrogel (■) and cells encapsulated within the PEGDA hydrogel (■). (*p<0.05).

stamp was implanted onto a chick embryo chorioallantoic membrane (CAM) to confirm its ability to create the patterned neovessels within tissue covered by the stamp.

First, the elastic modulus and swelling ratio of the PEGDA hydrogel were tuned to prepare a rigid and permeable hydrogel, so that the cell-encapsulated hydrogel would not only remain structurally stable at the implanted site but also support cellular activities. Increasing the total polymer concentration of the PEGDA hydrogel showed an increase in elastic modulus and a decrease in swelling ratio, which is the typical inverse relationship between stiffness and bulk permeability of conventional hydrogel systems (**Figure 1**a). In contrast, the hydrogel consisting of PEGDA and MA, which has multivalent methacrylic groups and hydrophilic hydroxyl groups,[11] showed an increase in both elastic modulus and swelling ratio with increasing mass fraction of MA (Figure 1a). The role of MA in increasing the swelling ratio of the hydrogel was further examined by monitoring water uptake into a hydrogel at non-equilibrium state using magnetic resonance imaging (MRI). Despite the higher stiffness of the PEGDA-MA hydrogel compared to the PEGDA hydrogel, water diffused into the PEGDA-MA hydrogel more rapidly (Figure 1b).

Subsequently, fibroblasts were encapsulated into the PEGDA and PEGDA-MA hydrogels via in situ photo cross-linking reaction with SLA unit (Figure S1).[12] Cells encapsulated into the PEGDA-MA hydrogel exhibited higher viability than those encapsulated into the PEGDA hydrogel, as confirmed with the larger intracellular cleavage of yellow tetrazolium salt (MTT) into a purple formazan product (Figure 1c). In addition, fibroblasts exposed to a 12-O-tetradecanoylphorbol-13-acetate, protein kinase C (PKC) activator, were stimulated to express multiple angiogenic factors, including vascular endothelial growth factor (VEGF) and Endothelin-1 (Figure S2a).[13] The cellular expression levels of VEGF and Endothelin-1 in the PEGDA-MA hydrogel were higher and more sustained than those encapsulated in the pure PEGDA hydrogel (Figure 1d & S2b).

Next, we introduced cylindrical microchannels (pores) into the PEGDA-MA hydrogels to localize cell-secreted angiogenic factors within the circular patterns (**Figure 2**). To determine the appropriate microchannel geometry, we estimated the dependency of the amount of angiogenic factors released through the channels on the microchannel diameter as follows. Assuming that the molar flux of angiogenic factors into the microchannel is J (depicted by the horizontal arrows in the side view of Figure 2a), and that there is no consumption of angiogenic factors in the channel, the average molar flux to be delivered to the tissue through the bottom of the channel, $J_{channel}$, would be

$$J_{channel} = \frac{\pi d H}{\pi d^2/4} \times J \quad (1)$$

where d is the diameter of the channel, and H is the height of the stamp. Therefore, the flux of angiogenic factors enhanced with the microchannels is

$$\frac{J_{channel}}{J} = \frac{4H}{d} \quad (2)$$

Hence, for a stamp with a thickness of 200 μm, this simple scaling law predicts that the enhancement of flux increases as the diameter of the microchannels decreases (Figure 2b).

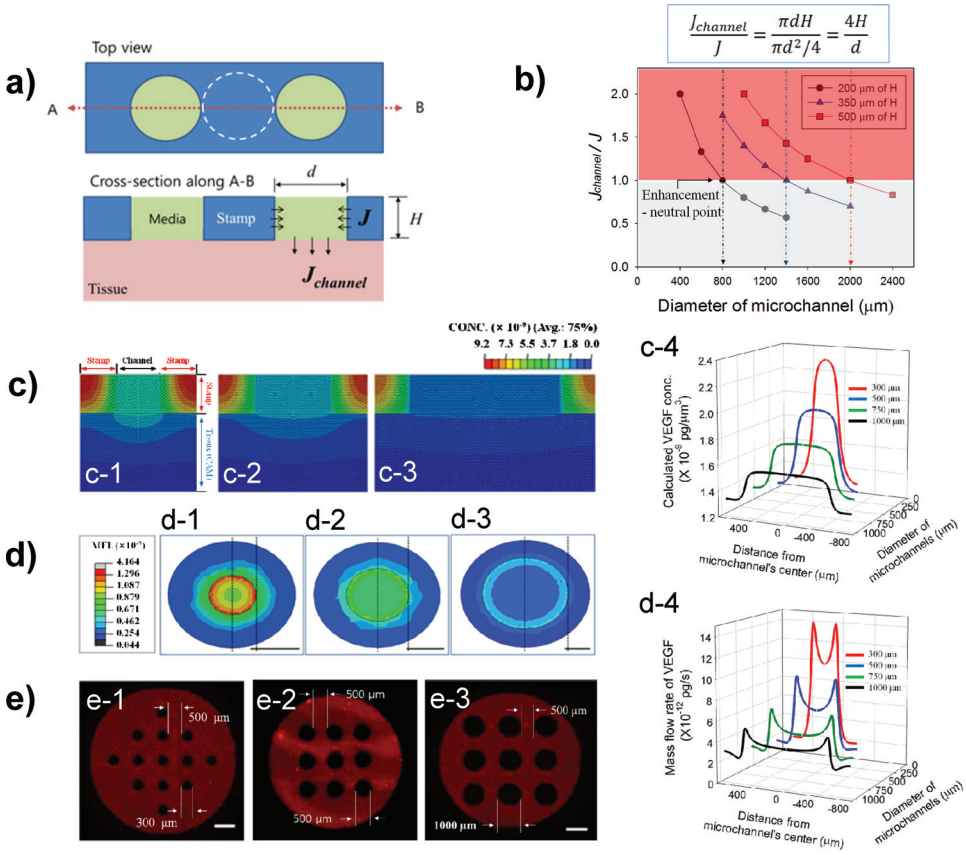

Figure 2. Stereolithographic incorporation of microchannels into a hydrogel. a) Schematics of top and side views of the microvascular stamp assembled to present microchannels with controlled diameter (d). b) A scaling law suggested that the average molar flux (J) to be delivered to the tissue through the bottom of the channel, $J_{channel}$, is enhanced, as the microchannwel diameter becomes smaller than 800 μm for a hydrogel with thickness of 200 μm. c) Numerical analysis of cross-sectional contours of VEGF concentration distributions at Day 7 for three different microchannel diameters (c-1: 300 μm, c-2: 500 μm, and c-3: 1000 μm). d) Numerical analysis of the top view of the mass flow rate of VEGF on a plane 20 μm below the hydrogel stamp-CAM interface. Scale bars represent 300 μm. Plots show the numerical values of VEGF concentration distributions (c-4) and mass flow rates (d-4) across the diameter of the channel at 20 μm below the stamp-tissue interface. e) Pictures of the hydrogel stamp with microchannels varied from 200 (c-1), to 500 (c-2), and 1,000 μm (c-3).

A microchannel of 800 μm diameter would be enhancement-neutral, i.e., would neither increase nor decrease the average amount of angiogenic factors delivered to the tissue through the channels. This critical microchannel diameter increases with thickness of the stamp (Figure 2b).

To validate the scaling law, a finite element model was created to simulate the molar flux of cell-secreted growth factors from the hydrogel with microchannels. The boundary conditions of the model are the constant production of VEGF molecules per unit volume in the hydrogel, with no diffusional flow or loss through the top of the gel. The diffusional flows in the hydrogel, microchannels, and within the tissue were presumed to be governed by the diffusion coefficients following Fick's law of diffusion. The diffusion across the hydrogel-channel, channel-tissue, and hydrogel-tissue interfaces were estimated by taking the average values of the diffusion coefficients of the two neighboring materials (for more details, see Supporting Information).

The simulation results clearly show that the concentration of VEGF below the smaller-diameter microchannel is much greater than that below the larger-diameter microchannel (Figure 2c). The concentration of VEGF directly below the stamp is lower than that below the channel, regardless of the difference of the microchannel diameter. This is due to the very slow diffusional rate in the hydrogel stamp compared to that in the media inside the microchannels. The media acts as a route for the VEGF to move along the entire inner surface of the channel, with a much higher diffusion rate at the surface of the tissue. In addition, there is an increased mass flow rate at the circumference of the microchannels (Figure 2d).

To validate the scaling law and numerical analysis, microchannels with diameters varied from 300, 500, to 1000 μm were fabricated in the PEGDA and PEGDA-MA hydrogels encapsulated with fluorescently labeled bovine serum albumin (BSA) (Figure 2e). Incorporation of the microchannels into the hydrogel made minimal difference in the elastic modulus and swelling ratio as compared to the microchannel-free hydrogel. Therefore, the original diameter of the microchannels was minimally affected during the in vitro incubation. To emulate the stamp being implanted on tissue, the hydrogel stamp was placed on the poly(acrylamide) hydrogel modified with succinimidyl ester groups that are chemically reactive to the amine

groups of BSA molecules (Figure S3). The hydrogel stamp containing microchannels with diameters of 300 and 500 μm, at which $J_{channel}$ is predicted to be larger than J, localized the BSA molecules in the microchannels (Figure S3). In contrast, a microchannel with diameter of 1,000 μm, at which $J_{channel}$ is predicted to be smaller than J did not exhibit the localization of proteins neither around nor within the circular pattern.

Finally, the hydrogel-based vascular stamps with controlled microchannels were implanted onto chick chorioallantoic membrane (CAM). Prior to their implantation, all hydrogels were incubated in media supplemented with the PKC activator for 24 hours, in order to stimulate cellular expression of angiogenic factors. Implantation of the PEGDA hydrogel with cells onto the CAM stimulated inflammation within two days, most likely because of the low cell viability and extravasation of the debris from the dead cells (Figure S5a). In contrast, the PEGDA-MA hydrogel minimally stimulated host inflammation, most likely because of its ability to increase the viability of encapsulated cells. Implantation of the PEGDA-MA hydrogel containing microchannels of diameter smaller than 800 μm stimulated the growth of neovessels with blood flow along its circular pattern (**Figure 3**a-2, 3a-3, 3b-2, and 3b-3). The spacing between the circular neovessels was 500 or 1000 μm which was the same as the spacing of the microchannels introduced into the hydrogel (Figure 3 and S5e). The cells encapsulated in the stamps remained viable at the implant sites. In addition, the circularly patterned neovessels were interconnected to each other, which suggested that sprouting of new capillaries from one circular-shaped neovessels stimulated formation of the neighboring patterned neovessels. The reproducibility of patterning neovessels was maintained at approximately 100% (Figure S6). The vascular stamp embedded in an endothelial cell-encapsulating collagen gel also resulted in the formation of patterned blood vessel-like tubules (Figure S7). Such patterning of neovessels was neither achieved in the same hydrogel without cells, in that loaded only with VEGF, nor in the microchannel-free hydrogel loaded with cells (Figure S5). In addition, none of the neovessels replicated the circular pattern of microchannels when the diameter of the microchannels was increased to 1,000 μm (Figure 3a-4 and b-4). Most of the neovessels were formed along irregular and tortuous paths.

Accordingly, the vascular stamp containing microchannels with diameter of 500 μm resulted in a significant increase in the number and size of mature neovessels at the implantation site, as compared to the microchannel-free control conditions and the hydrogel containing microchannels with diameter of 1000 μm

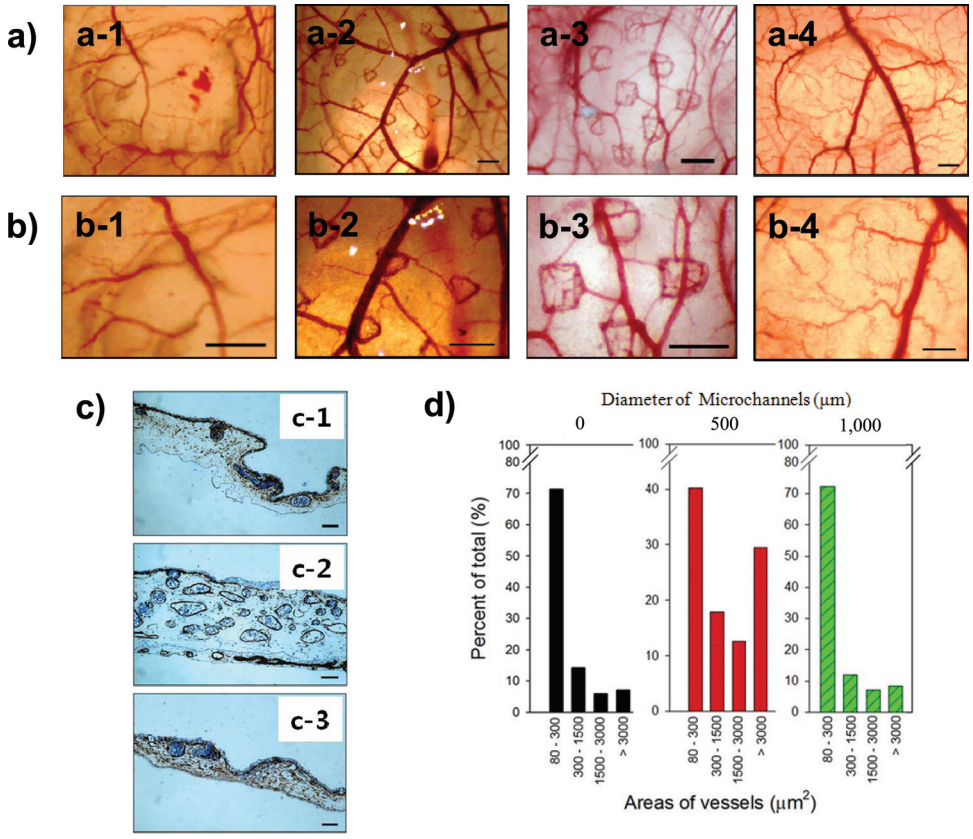

Figure 3. Formation of patterend neovessels on chick chorioallantoic membrane (CAM). a) The bright field images of neovessels formed under PEGDA-MA hydrogels containing microchannels of diameters at 0 (a-1), 300 (a-2), 500 (a-3), and 1,000 μm (a-4). The implant sites shown in (a) were further magnified in (b) (scale bars represent 500 μm). These images were captured seven days after implantation. c) The histological images of mature neovessels positively stained by an antibody to α-smooth muscle actin (α-SMA) (scale bars represent 100 μm). Photos (c-1), (c-2) and (c-3) represent cross-sections of CAM implanted with hydrogels containing microchannels with diameter of 0 (c-1), 500 (c-2), and 1,000 μm (c-3). d) The cross-sectional area of blood vessels was mediated by diameters of microchannels.

(Figure 3c). The vascular stamp resulted in the 2.5-fold increase of the thickness of CAM, as compared with CAM implanted with other controls. The size analysis of the blood vessels exhibited that the microchannels with diameter of 500 μm significantly stimulated formation of arterioles with vessel area of over 1000 μm^2 (i.e., 40% of total blood vessels in CAM) (Figure 3d).

Overall, our results demonstrate that the microvascular stamp created mature and functional neovessels with desired patterns in live tissue. Ultimately, the microvascular stamp could increase the vascular size and density at an implant site. Such refined patterning of blood vessels through which blood flows has to date never been reported. One interesting feature of the vascular stamp is the capability to enable cells to retain their viability and growth factor production in a PEGDA-MA hydrogel system. We propose that MA in the PEGDA-MA hydrogel is a key factor because hydrophilic MA enhances the transport of oxygen and nutrients into the hydrogel.[15,16] Therefore, the resulting PEGDA-MA hydrogel would greatly overcome the challenges encountered with current hydrogel design, which is often plagued by the inverse dependency between stiffness and permeability. This enhanced transport property can be further modulated by controlling size distribution of nanometer-sized pores in hydrogels with the molecular weights of PEGDA or MA.[17]

Another highlight of the vascular stamp was its ability to localize angiogenic factors in a pre-defined pattern using microchannels stereolithographically incorporated into the gel. According to the diffusion-based scaling law and the numerical analysis, the molar flow rate of angiogenic factors into the tissue beneath the circumference of the microchannel wall was increased with the use of the appropriate microchannel dimension. We propose that the local increase of the mass flow rate of angiogenic factors at the edge of the microchannel wall may be a key factor to determine whether blood vessels are able to grow in the circular pattern. As a newly formed blood vessel actively consumes angiogenic factors, regions that have a high mass flow rate and faster replenishment of angiogenic factors would stimulate the continued growth of a mature blood vessel.[18,19]

In addition, when only VEGF was incorporated in the hydrogel, no patterning of the neovessels occurred, which suggests the importance of the constant production of multiple growth factors in generating mature and functional blood vessels in the desired patterns. It is also possible that VEGF may be denatured during the in situ cross-linking reaction activated by the high intensity laser. Therefore, live cells may provide an improved method for patterning the neovessels, because of their intrinsic properties of synthesizing and secreting multiple angiogenic factors in a sustained manner. We also hypothesize that the sustained delivery of angiogenic factors increases the vascular size as well as vascular density, although this aspect needs to be confirmed in future studies.[20,21]

In the end, controlling the "bottom-up" emerging behavior of the neovessel formation via "directed top-down" cues using the "living" microvascular stamp can be a major step forward to better understanding and engineering the development of neovessels and further improving treatment of various injuries, traumas, and diseases. For example, neovessels patterned by a microvascular stamp will be discernable from other pre-existing neovessels, so the roles of normal or pathologic extracellular microenvironment in development, homeostasis, and remodeling of neovessels can be better understood. The microvascular stamp can also be implanted in ischemic tissues to engineer mature neovessels with regular spacing and subsequently improve recovery of tissue and organ functions. Finally, the design principles established to assemble the microvascular stamp will be useful in designing a broad array of bioimplants and tissue engineering scaffolds to create "on demand" microvascular networks in an organized fashion.

Experimental Section

An expanded procedures is provided in the Supporting Information. In brief, gel-forming polymers, poly(ethylene glycol) diacrylate (PEGDA) and methacrylic alginate (MA), were synthesized as described in Supporting information and in our previous work.[11] The PEGDA and MA dissolved in Dulbecco's modified Eagle's medium (DMEM, Sigma Aldrich) were mixed at varied mass ratios, while keeping the total polymer concentrations constant. The pre-gel solution was subsequently placed into the dish at the center of the platform in SLA.[12] The SLA process was repeated until completion of the 3D assembly of the hydrogel (for more detail, see Figure S1). For cell encapsulation, the mixture of NIH/3T3 cells (ATCC) (5.0×10^6 cells/mL) and pre-gel solution was exposed to the laser of SLA to activate hydrogel formation (for more details, see Supporting Information).

The hydrogel stiffness was evaluated with measurement of the elastic modulus of a hydrogel using a mechanical testing system (MTS Insight). The hydrogel swelling ratio at equilibrium was determined by measuring the weight of the hydrated gel after 24 hours in neutral buffered solution at 37 °C and that of the dried gel. The hydrogel permeability was also evaluated by monitoring water uptake into a hydrogel at non-equilibrium state with the magnetic resonance imaging (600 MHz Varian Unity/Inova nuclear magnetic resonance (NMR) spectrometer (14.1 T Magnet) (for more details, see Supporting Information).

An axisymmetric finite element model was created using Abaqus/CAE version 6.8 - 4 (for more details, see Supporting Information).

The function of microvascular stamp to engineering neovessels pattern was examined by implanting the cell-hydrogel construct onto chicken chorioallontoic membrane (CAM) according to a previously developed method.[22] Fertilized chicken eggs (Hy-Line W-36) were obtained from the University of Illinois Poultry Farm (Urbana, IL) (for more details, see Supporting Information).

Statistical significance was determined using one-way ANOVA followed by Tukey's Multiple Comparison Test ($p < 0.05$).

Supporting Information

Supporting Information is available from the Wiley Online Library or from the author.

Acknowledgements

This work was supported by US Army Telemedicine & Advanced Technology Research Center (W81XWH-08-1-0701), National Science Foundation (CAREER: DMR-0847253, STC-EBICS Grant CBET-0939511, IGERT DGE-0965918), American Heart Association (Scientist Development Grant 0830468Z) and the Amore Pacific Corporation (South Korea). The authors also wish to thank Prof. Soonnam Oh, M.D., Ph.D., at the Catholic University of Korea for her discussions.

Received: August 19, 2011
Published online: November 23, 2011

[1] A. Dorfleutner, P. Carmeliet, B. M. Mueller, M. Friedlander, W. Ruf, *Nat. Med.* **2004**, *10*, 502.
[2] P. Carmeliet, R. K. Jain, *Nature* **2000**, *407*, 249.
[3] Y. Dor, V. Djonov, E. Keshet, *Trends Cell Bio.* **2003**, *13*, 131.
[4] R.-R. Chen, E.-A. Silva, W.-W. Yuen, D.-J. Mooney, *Pharm. Res.* **2007**, *24*, 258.
[5] E.-A. Silva, D.-J. Mooney, *Biomaterials* **2010**, *31*, 1235.
[6] S. M. Kim, S. B. Moo, S. J. Hwang, *Tissue Eng. Regen. Med.* **2008**, *5*, 959.
[7] A. Khademhosseini, R. Langer, J. Borenstein, J. P. Vacanti, *Proc. Natl. Acad. Sci. USA* **2005**, *103*, 2480.
[8] U. Gbureck, T. Holzel, C. J. Joillon, F. A. Muller, J. E. Barralet, *Adv. Mater.* **2007**, *19*, 795.
[9] I. Barkefors, S. Thorslund, F. Nikolajeff, J. A. Kreuger, *Lab Chip* **2009**, *9*, 529.
[10] R. J. DeVolder, H. Bae, J. Lee, H. J. Kong, *Adv. Mater.* **2011**, *23*, 3139.
[11] C. Cha, S. Kim, L. Cao, H. J. Kong, *Biomaterials* **2010**, *31*, 4864.
[12] V. Chan, P. Zorlutuna, J. H. Jeong, H. J. Kong, R. Bashir, *Lab Chip* **2010**, *10*, 2062.
[13] S. Grugel, G. Finkenzeller, K. Weindel, B. Barleon, D. Marme, *J. Biol. Chem.* **1995**, *270*, 25915.
[14] K. Park, L. J. Millet, N. Kim, H. Li, X. Jin, G. Popescu, N. Aluru, K. J. Hsia, R. Bashir, *Proc. Natl. Acad. Sci. USA* **2010**, *107*, 20691.
[15] D.-E. Discher, D.-J. Mooney, P.-W. Zandstra, *Science* **2009**, *324*, 1673.
[16] D.-R. Albrecht, G.-H. Underhill, T.-B. Wassermann, R.-L. Sah, S.-N. Bhatia, *Nat. Methods* **2006**, *3*, 369.
[17] J. Wang, A. D. Gonzalez, V. M. Ugaz, *Adv. Mater.* **2008**, *20*, 4482.
[18] R.-H. Adams, K. Alitalo, *Nat. Rev.* **2007**, *8*, 464.
[19] E.-M. Conway, D. Collen, P. Carmeliet, *Cardiovasc. Res.* **2001**, *49*, 507.
[20] J.-A. Burdic, M.-N. Mason, A.-D. Hinman, K. Thorne, K.-S. Anseth, *J. Control. Release* **2002**, *83*, 53.
[21] M.-P. Lutolf, J.-A. Hubbell, *Nat. Biotechnol.* **2005**, *23*, 47.
[22] C.-A. Staton, C. Lewis, R. Bicknell, in *Angiogenesis Assays: A critical appraisal of current techniques*, Wiley, New York **2007**, Ch. 11.

ADVANCED MATERIALS

Supporting Information

for Adv. Mater., DOI: 10.1002/adma.201103207

"Living" Microvascular Stamp for Patterning of Functional Neovessels; Orchestrated Control of Matrix Property and Geometry

*Jae Hyun Jeong , Vincent Chan , Chaenyung Cha , Pinar Zorlutuna , Casey Dyck , K. Jimmy Hsia , Rashid Bashir , * and Hyunjoon Kong **

Supporting Information

Synthesis of MA and PEGDA. For the synthesis of methacrylic alginate (MA), 2-aminoethyl methacrylate was conjugated to the carboxylate group of alginate via EDC chemistry. The alginate used in this experiment (molecular weight (M_w) ~ 50,000 g/mol) was obtained by irradiating alginate rich in gluronic acid residues, (LF20/40, FMC Technologies, M_w ~ 250,000 g/mol) with a dose of 2 Mrad for 4 hours from a ^{60}Co source. The irradiated alginate was dissolved in the 0.1 M MES ((2-(N-morpholino) ethanesulfonic acid) buffer (pH 6.4, Sigma-Aldrich) at the concentration of 1.0 % (w/v). Then, 1-hydroxybenzotriazole (HOBt, Fluka), 1-ethyl-3-(3-dimethylaminopropyl) carbodiimide (EDC, Thermo Scientific) and 2-aminoethyl methacrylate (AEMA, Sigma Aldrich) were dissolved in the alginate solution and stirred for 18 hours. Both the molar ratio of HOBt to AEMA and the molar ratio of EDC to AEMA were kept constant at 2:1. The mixture was dialyzed extensively against deionized (DI) water for three days, while exchanging the DI water every 12 hours. The dialyzed alginate solution was lyophilized, and reconstituted to a 3 wt % stock solution. The conjugation of methacrylate groups onto the alginate was confirmed by ^{1}H-NMR (300MHz, QE300, General Electric), as previously reported. In this study, the number of methacrylates linked to a single alginate with molecular weight (M_w) of 50,000 g/mol was kept constant at 60. In parallel, poly(ethylene glycol) diacrylates (PEGDA) was synthesized via chemical reaction between poly(ethylene glycol) (PEG, Sigma Aldrich) and acryloyl chloride (Sigma Aldrich). First, PEG was dissolved in dichloromethane at the concentration of 10 wt %. Next, acryloyl chloride and triethylamine (Fisher Chemical) were dissolved in the PEG solution and stirred overnight under dry N_2 gas. The molar ratio of PEG, acryloyl chloride and triethylamine was 1:4:4. Finally, the insoluble salt (triethylamine-HCl) was filtered, and the product was precipitated by adding ice-cold ether. The crude product was dissolved into DI water and dialyzed for one day to remove unreacted starting materials and the salt, a byproduct. Then, the product was frozen at -20 ºC and lyophilized. The conjugation of acrylate groups onto PEG was confirmed by ^{1}H-NMR (300 MHz, QE300, General Electric).

Magnetic Resonance Imaging (MRI) of the Hydrogel. Spin echo multi-slice (SEMS) pulse sequence for MR imaging of the hydrogel was used to acquire resonance data, which were then converted into water density map using VNMR 6.1C software. For SEMS pulse sequence, the repetition time (T_R) of 2.5 s and the echo time (T_E) of 5 ms were used. The field of view (FOV) was 1.6 x 1.6 cm, and the image matrix was 128 x 64 pixels. The resulting water density images were processed to present the density spectrum for comparison using MATLAB (The Mathworks^{TM}). For visualization, pseudo-color was added to the images using the ImageJ software (free image analysis software from National Institutes of Health). For counting water intensity peaks, the rectangular gel picture from the image was selected, and the histogram of the image (count vs. color intensity) was taken using the ImageJ software.

Experimental set-up to examine localization of proteins diffused from the hydrogel with microchannels. The microscopic platform was prepared on a cover glass. Following the treatment with 0.1 M sodium hydroxide, the coverslip was siliconized with 3-

aminopropyltriethoxy silane (APES, Sigma) followed by modification with 0.5% glutaraldehyde (Sigma) in PBS. The 1.0 mL of pre-gel solution was prepared with 200 μL of 40 % (w/v) acrylamide (AAm, Aldrich), 132 μL of 2 % (w/v) bis-acrylamide (Bis, Aldrich), 50 μL of 10 % ammonium persulfate (APS, Aldrich) and 2 μL of N′,N′,N′,N′-tetramethylethylene-diamine (TEMED, Aldrich) in DI water. Then, the pre-gel solution was sandwiched and allowed to polymerize between the modified coverslip and unmodified coverslip of 22 mm diameter for 10 minutes at room temperature. After the polymerization, the unmodifed cover glass was removed, and the poly(acrylamide) (PAAm) gel-coated cover glass was rinsed twice. The surface of PAAm was functionalized with -NHS (-succinimidyl) groups by activating with *N*-sulfosuccinimidyl-6-[4′-azido-2′-nitrophenylamino] hexanoate (Sulfo-SANPAH, Pierce) in the presence of UV light. UV with 252 nm wavelength was exposed twice for 7 minutes on the Sulfo-SANPAH solution on PAAm. The fluorescent Bovine Serum Albumin (rhodamine-BSA, Aldrich) as a model protein was encapsulated in the PEGDA-MA hydrogel containing microchannels, and the hydrogel was placed on the activated PAAm substrate. The BSA diffuse onto the –NHS (-succinimidyl) groups on the PAAm gel surface during incubation overnight. BSA reacts with –NHS groups to form covalent bonds, and the fluorescence pattern under the PEGDA-MA hydrogel was examined using the fluorescent microscope.

Numerical Analysis. An axisymmetric finite element model was created using Abaqus/CAE version 6.8 - 4. It was assumed that the diffusional flow effects of each microchannel had a negligible impact on the neighboring microchannels and therefore the modeling focused on an individual microchannel of varying diameter. Only the radius of the hole and the corresponding area of the tissue would be changed from one model to the next. The size of hydrogel stamp used in the model was held constant at 250 μm in width and 200 μm in height to correspond with the experimental stamp height and spacing between channels. A mesh was created with microchannel with diameters of 300, 500, 750, and 1,000 μm using 3 node axisymmetric triangles. The top surface of the model was assumed to have no diffusional flow or loss through the top of the gel and microchannel as was dictated by the experimental setup. The outer vertical surface was also assumed to have no diffusional flow in the horizontal direction outside of the control volume. The CAM membrane was modeled as being 400 μm thick with a constant concentration of zero at the lower boundary of the model. This constant concentration acted as a sink, thereby consuming the VEGF once it reached the bottom surface of the model. The diffusion calculations were governed by Fick's law of diffusion with diffusion coefficients of 200 $\mu m^2/s$, 1.0 $\mu m^2/s$, and 0.1 $\mu m^2/s$ for the media, CAM, and hydrogel stamp, respectively (1). The diffusion across the boundaries between different materials was assumed to be unobstructed. The diffusion coefficient for each of the boundaries was subsequently set as the average of the two materials involved. The stamp had a constant body flux of 3.1×10^{-14} $pg/\mu m^3\cdot s$ which represented the constant production of VEGF by the fibroblasts (Fig. 2*D*). All simulations were in micrometers, seconds, and picograms. Each of the diameters was modeled to simulate a period of 7 days.

Cell Encapsulation. NIH/3T3 cells (ATCC) were expanded and passaged at 37 °C with 5 % CO_2 in Dulbecco's modified Eagle's medium (DMEM, ATCC) supplemented by 10 % fetal

bovine serum (FBS, ATCC), and 1 % penicillin/streptomycin (ATCC). All the cells before the passage number of 10 were used in this study. Prior to encapsulation in hydrogels, cells were mixed with the pre-gel polymer solution. The cell density was kept constant at 2.0×10^6 cells/ml. The mixture of cell and pre-gel solution was exposed to the laser of SLA to activate hydrogel formation. The cell-hydrogels were incubated in DMEM supplemented by 10 % fetal bovine serum (FBS), while changing the media every two days. On days 0, 1, 3, 5, and 7, viability of cells encapsulated into the hydrogel was quantitatively evaluated using a MTT [(3-(4,5-dimethylthiazol-2-yl)-2,5-diphenyltetrazolium bromide) reagent (ATCC)] assay kit. The encapsulated cells were stimulated to secret growth factors by adding 0.2 mL of DMEM and 100 ng/ml of 12-O-Tetradecanoylphorbol-13-acetate (TPA, ATCC) reagent into a well of a 96-well plate which contains each cell-encapsulating gel. After incubating the cell-hydrogel construct for 24 hours, 100 µl of cell culture media was mixed with a cocktail of biotinylated detection antibodies, and incubated overnight with the proteome profiler mouse angiogenesis array (R&D Systems). The array membrane was washed to remove unbound material and streptavidin-Fluor® (430) conjugates (Invitrogen) and positively stained spots were imaged using a Phosphor Imager (Bio-Rad). In addition, on days 1, 3, and 5, the amount of VEGF secreted by cells was quantitatively evaluated by the sandwich enzyme immunoassay technique using the mouse VEGF Immunoassay kit (R&D Systems). The sample containing VEGF was pipetted into a well where a polyclonal antibody specific for mouse VEGF has been pre-coated and incubated for 2 hours. After washing away any unbound substances, an enzyme-linked polyclonal antibody specific for mouse VEGF was added to the well. The enzyme reaction yielded a blue-colored product, and the color intensity was measured using a microplate absorbance reader (Synergy HT, Biotek). The measured value was converted to the amount of VEGF using a calibration curve. The amount of VEGF was further normalized by the number density of cells initially encapsulated into each hydrogel.

Chorioallontoic Membrane (CAM)-Based Angiogenesis Assay. The function of microvascular stamp to engineering neovessels pattern was examined by implanting the cell-hydrogel construct onto chicken chorioallontoic membrane (CAM). Following the initial incubation, a small window (1.0 × 1.0 cm) was created on top of each egg shell. Then, a freshly fabricated fibroblasts-encapsulating hydrogel disk (5×10^6 cells/ml) was implanted on top of the CAM of individual embryos. At days 0, 2, 4 and 7 after implantation, CAM images were captured using a S6E stereomicroscope (Leica) linked with D-Lux E Camera (Leica). In parallel, the fixed membrane was also embedded in paraffin and the cross-section was stained for α-smooth muscle actin (α-SMA Immunohistology Kit, Sigma-Aldrich) to count the number of mature blood vessels.

Supporting Figures

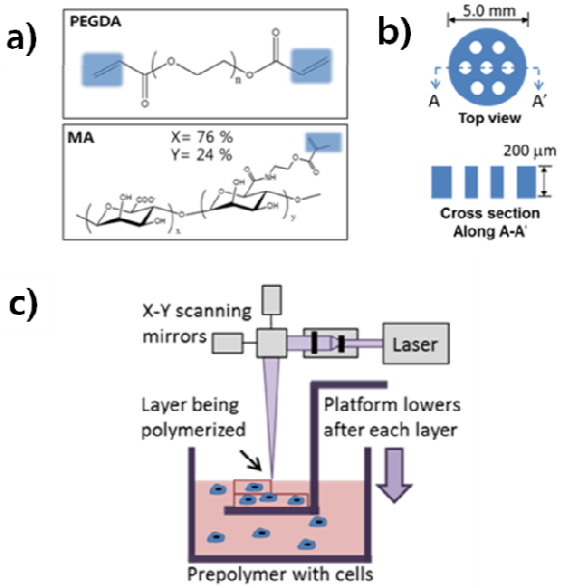

Figure S1. (a) Molecular structures of poly(ethylene glycol) (PEGDA) and methacrylic alginate (MA). (b) Schematic diagram of the stamp prepared with stereolithographic assembly. (c) Bottoms-up process for cell-encapsulated hydrogel assembly. The hydrogel with microchannels was fabricated by photo crosslinking the mixture of cell and pre-gel solution in a layer by layer fashion using a stereolithography apparatus (SLA, Model 250/50, 3D Systems). In this study, a commercially-available SLA was modified to accommodate for the bottoms-up approach as described in our previous work. In the bottoms-up approach, the pre-gel solution is pipetted into the container one layer at a time from the bottom to the top. This setup was designed to reduce total volume of photopolymer in use and also remove photopolymers used from static conditions. 3D computer-aided design (CAD) models were generated using AutoCAD 2009 (Autodesk) and exported to stereolithography (SLA) format for creating hydrogels containing microchannels. The SLA software, 3D Lightyear v1.4 (3D system), was used to slice the 3D models into a series of 2D layers from a user-specified thickness. The laser was used to selectively crosslink the pre-gel solution at a precisely calculated energy dose. The elevator controlled by the SLA was lowered by a specified distance, and the part was recoated.

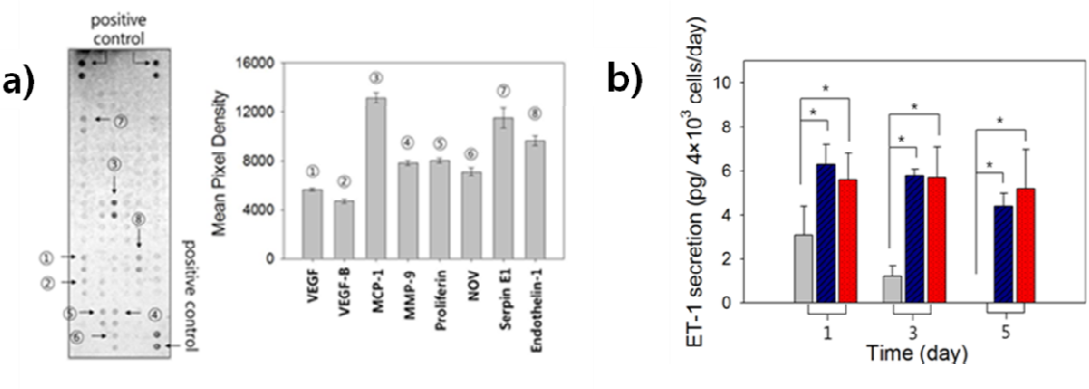

Figure S2. (a) Angiogenic growth factors including VEGF, VEGF-B, MCP-1, MMP-9, proliferin, NOV, Serpin E1 and Endothelin-1 were secreted from NIH/3T3 fibroblasts encapsulated within a PEGDA-MA hydrogel, following exposure of cells to an activator of protein kinase C. (b) On Days 1, 3, and 5, the cellular secretion level of Endothelin-1 was measured using the mouse Endothelin-1 (ET-1) Immunoassay kit (Enzo Life Sciences). The cells encapsulated within the PEGDA-MA hydrogels without microchannels (▬) and with microchannels (▬) expressed the larger amount of endothelin-1 than those within the PEGDA hydrogel (▬). The values of ET-1 secretion from the PEGDA-MA hydrogel without microchannels and from the PEGDA-MA hydrogel with microchannels were statistically different from that from the PEGDA hydrogel (*$p<0.05$).

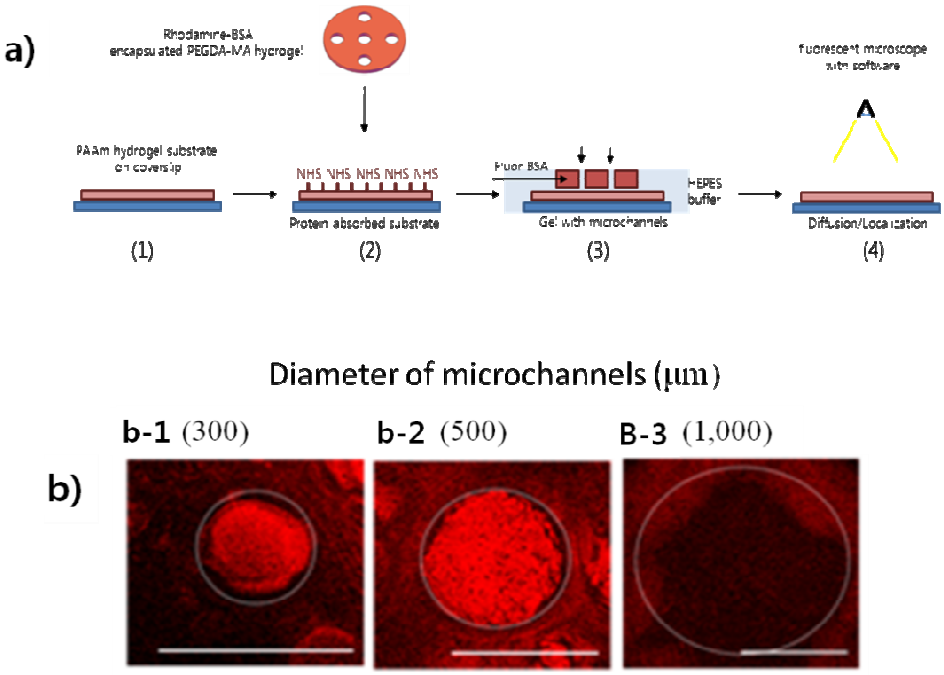

Figure S3. (a) Schematic of the experimental set-up to examine localization of proteins diffused from the hydrogel with microchannels. The poly(acrylamide) (PAAm) gel-coated microscopic platform was prepared on a cover glass (1). The surface of PAAm was functionalized with -NHS (-succinimidyl) groups (2). The hydrogel containing the fluorescent Bovine Serum Albumin (BSA) was placed on the activated PAAm substrate. The BSA diffuse onto the –NHS (-succinimidyl) groups on the PAAm gel surface during incubation overnight (3). BSA reacts with –NHS groups to form covalent bonds, and the fluorescence pattern under the PEGDA-MA hydrogel was examined using the fluorescent microscope (4). (b) The hydrogel stamp was placed on a poly(acrylamide) hydrogel modified with succinimidyl ester groups. The BSA released from the hydrogel stamps containing microchannels with diameter of 300 μm (b-1) and 500 μm (b-2) was localized within the circular pattern. In contrast, the hydrogel containing a channel with diameter of 1,000 μm showed minimal localization of BSAs within the circular pattern (b-3).

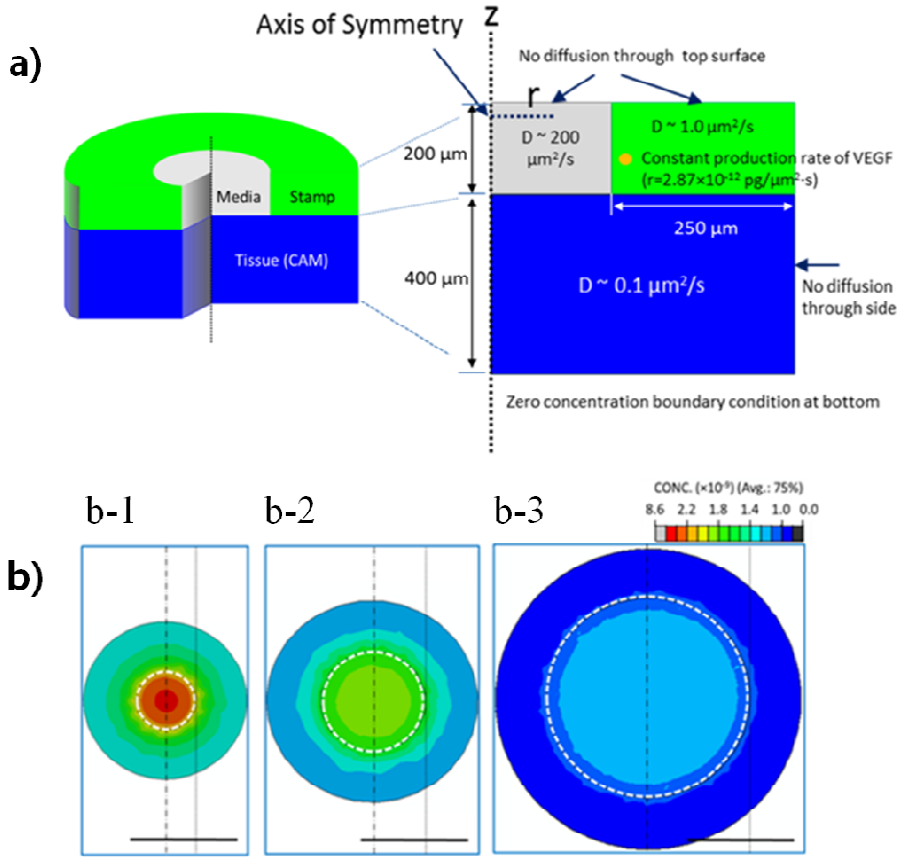

Figure S4. (a) Boundary conditions and the dimensions of the stamp used in the numerical analysis. The top surface and the outer vertical surface of the stamp were assumed to be insulated. The CAM membrane was modeled as being 400 μm thick with a constant concentration of zero at the lower boundary of the system. (b) Numerical analysis of the top view of the VEGF concentration distribution on a plane 20 μm below the hydrogel-CAM interface at Day 7 for three different microchannel diameters (b-1; 300 μm, b-2; 500 μm, and b-3; 1000 μm).

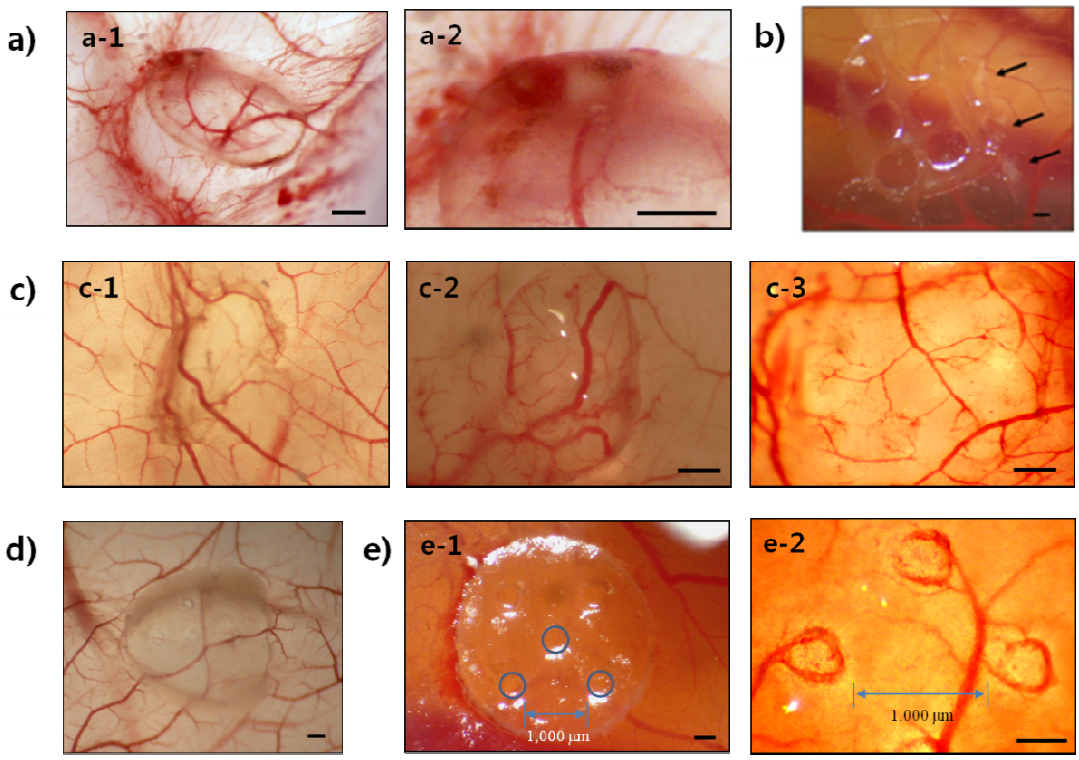

Figure S5. Chick embryo chorioallantoic membrane (CAM) angiogenesis assay. (a) Implantation of the PEGDA hydrogel did not generate capillary patterns, but instead stimulated inflammation. (b) The fractured hydrogel stimulated inflammation, marked by white fibrous tissues around the implant (indicated by an arrow), within two days, while the intact hydrogel only minimally stimulated host inflammation. (c) Patterning of neovessels was not achieved with the cell-free PEGDA-MA hydrogel incubated with PKC activator (c-1), or the hydrogel which contains encapsulated cells at densities of 5×10^4 cells/ml (c-2), and 5×10^5 cells/ml (c-3). (d) Encapsulating only VEGF (30 ng/ml) without fibroblasts did not generate any patterned neovessels. (e) The vascular stamp with a spacing of microchannels of 1.0 mm generated a circular pattern of neovessels with a spacing of 1.0 mm. Scale bars represent 500 μm.

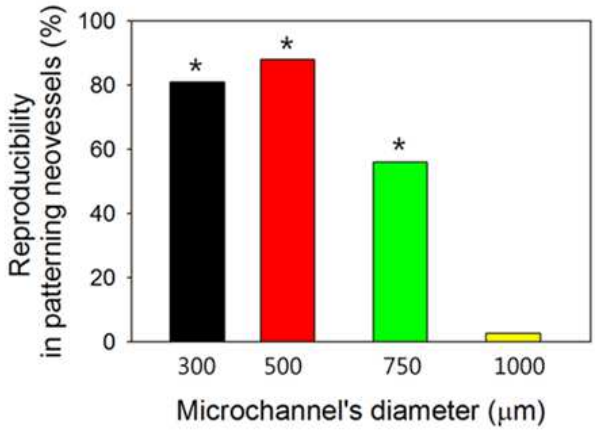

Figure S6. The reproducibility of patterning neovessels, quantified with the number ratio of the patterned neovessels to the microchannels, was related to the diameter of microchannels. The values of the reproducibility in patterning neovessels for microchannel diameters at 300, 500 and 750 μm were statistically different from that attained with microchannel diameter at 1,000 μm (*$p<0.05$). The values of reproducibility represent averaged values from four different samples/CAM assays for each microchannel diameter.

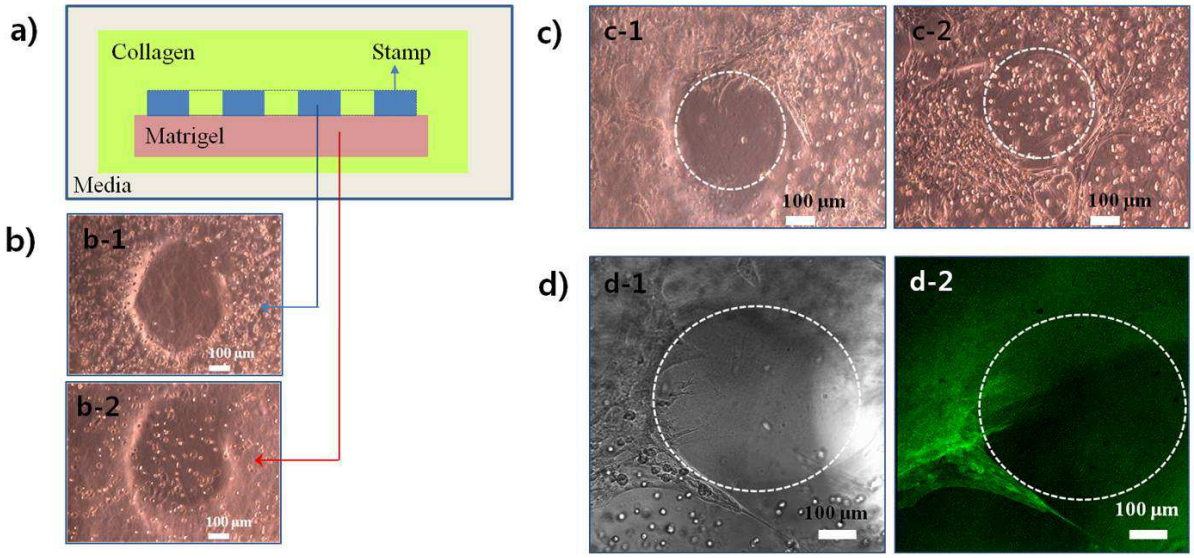

Figure S7. (a) Schematic of the experimental 3D assay to examine directed development of blood vessel-like tubules in 3D hydrogel. Briefly, endothelial cells (C166, ATCC) were cultured on growth factor-reduced (GFR) Matrigel on the MatTek dish. The cell density was kept constant at 5×10^6 cells/ml in each MatTek. The vascular stamp encapsulating fibroblasts was placed on the Matrigel and incubated at 37 °C for 30 minutes to allow it to attach to the Matrigel. Then, the whole gel system was completely embedded in a collagen gel by mixing collagen I solution (3.0 mg/ml, Puramatrix), Dulbecco's Modified Eagle Medium (DMEM, Cellgro), and reconstituting solution (0.26 M of sodium hydrogel carbonate, 0.2 M 4-(2-hydroxyethyl)-1-piperazineethanesulfonic acid, and 0.04 N of sodium hydroxide) at a ratio of 8:4:1. This mixture was subsequently incubated at 37 °C for 4 hours to form a 3D collagen hydrogel. Then, the spatial reorganization of endothelial cells in the 3D Matrigel was examined using the microscope. (b) The first image b-1 shows the fibroblast cells loaded in the vascular stamp, while the next image b-2 shows the endothelial cells loaded in the Matrigel. (c) The vascular stamp encapsulated in the collagen gel stimulated the migration of endothelial cells toward microchannels as shown in the image c-1 and subsequently formed circular patterns of blood vessel-like tubules under the circles of microchannels, as displayed in image c-2. In (c), the white dots represent microchannels in the vascular stamp. (d) Magnified views of image c-2. Image d-1 represents the bright field image of endothelial cells localized around the circumference of the microchannel, and image d-2 represents the endothelial cell lumen stained with fluorescein-phalloidin (green).